Numerical modeling of multiphase first-contact miscible flows. Part 2. Front-tracking/streamline simulation

Ruben Juanes[1] and Knut–Andreas Lie[2]

[1] Stanford University, Department of Petroleum Engineering
65 Green Earth Sciences Building, Stanford, CA 94305, USA

[2] SINTEF ICT, Department of Applied Mathematics
P.O. Box 124 Blindern, NO-0314 Oslo, Norway

Submitted to *Transport in Porous Media*

October 24, 2005

Abstract

In this paper we complete the description and application of a computational framework for the numerical simulation of first-contact miscible gas injection processes. The method is based on the front-tracking algorithm, in which numerical solutions to one-dimensional problems are constructed in the form of traveling discontinuities. The efficiency of the front-tracking method relies on the availability of the analytical Riemann solver described in Part 1 and a strategy for simplifying the wave structure for Riemann problems of small amplitude. Several representative examples are used to illustrate the excellent behavior of the front-tracking method. The front-tracking method is extended to simulate higher-dimensional processes through the use of streamlines. The paper presents a validation exercise for a quarter five-spot homogeneous problem, and an application of this computational framework for the simulation of miscible flooding in three-dimensional, highly heterogeneous formations. In this case, we demonstrate that a miscible water-alternating-gas injection scheme is more effective than waterflooding or gas injection alone.

KEY WORDS: porous media, miscible displacement, water-alternating-gas, Riemann problem, front-tracking, streamline simulation

1 Introduction

In this series of two papers we describe and apply a front-tracking/streamline method for the numerical simulation of multiphase first-contact miscible flows. Such flows occur in enhanced oil

recovery processes by gas injection, and environmental remediation of polluted aquifers.

The proposed formulation has three main components:

1. A complete, analytical Riemann solver.

2. A front-tracking scheme to solve general one-dimensional initial and boundary value problems.

3. A streamline simulation approach to solve three-dimensional problems in heterogeneous media, which decouples the 3D transport equations into a set of 1D problems along streamlines.

The analytical solution to the Riemann problem was described in Part 1 of the series [1]. The Riemann problem consists in solving a system of conservation laws in an infinite one-dimensional domain, with piecewise constant initial data separated by a single discontinuity. Our mathematical model makes several important assumptions: (1) it is a two-phase system, in which water is immiscible with the hydrocarbon phase, and the two hydrocarbon components (oil and solvent) mix readily in all proportions; (2) the fluids are incompressible and do not experience volume change upon mixing; (3) the effects of gravity and capillary forces are negligible; (4) the multiphase flow extension of Darcy's law is applicable; and (5) the effects of viscous fingering are negligible. Under these assumptions, the problem is described by a 2×2 hyperbolic system of conservation laws. In Part 1 we analyzed the mathematical character of the system and gave a complete analytical solution to the Riemann problem, using an analogy with the system of equations describing polymer flooding [2; 3].

Here, we use the analytical Riemann solver as a building block for constructing approximate (numerical) solutions using a front-tracking scheme. Front-tracking methods refer to numerical schemes that perform tracking of shocks and other evolving discontinuities [4]. They were developed to construct approximate and exact solutions to hyperbolic systems of conservation laws in one space dimension with general initial data [5], and they have been used as an essential tool in proving uniqueness of the solution [6]. Early application areas of the method include gas dynamics [7] and reservoir simulation [8]. Of particular interest is the work of Risebro and Tveito [9], where the front-tracking method is applied to the multicomponent polymer flooding system in one dimension. In our implementation of the front-tracking method, all waves are treated as discontinuities. Shock waves and contact discontinuities are tracked exactly, and rarefaction waves are approximated by small inadmissible shocks. The discontinuities are tracked until they interact and define a new Riemann problem. The approximate solution of this new Riemann problem leads to a new set of additional discontinuities that need to be tracked. Repeated application of this procedure allows marching in time. The main advantages of the front-tracking method just described are: (1) it captures discontinuities exactly without introducing any numerical diffusion; (2) it is grid-independent; (3) it is unconditionally stable; and (4) it can be very efficient if an analytical Riemann solver is available.

In this paper, we propose the use of streamlines to perform numerical simulation of miscible flooding in higher-dimensional, heterogeneous media. Streamline methods are based on a staggered solution of a global pressure equation and the system of transport equations [8; 10; 11]. Solution of the pressure equation defines the velocity field used to trace the streamlines. In this way, streamline methods decouple the three-dimensional equations describing the transport

of individual components into a set of one-dimensional problems along streamlines. With a proper parameterization of the streamlines, the numerical solution is then obtained using the front-tracking method described above. This computational framework was employed by the authors for the simulation of immiscible three-phase flow [12; 13], and it is extended here to miscible gas injection problems. The method is therefore fundamentally different from that of Holden and Risebro [14] and Haugse et al. [15], where front-tracking is applied in conjunction with operator-splitting, and one-dimensional problems are solved sequentially in each spatial dimension.

An outline of the paper is as follows. The front-tracking algorithm is given and discussed in Section 2. In Section 3 we present several representative one-dimensional simulations that illustrate the excellent behavior of the front-tracking method. In Section 4 we study the convergence behavior of the method for a two-dimensional problem in a homogeneous medium, and present an application of the proposed computational framework to the simulation of miscible flooding in a three-dimensional, highly heterogeneous formation. We compare recovery predictions for different injection scenarios, and conclude that a miscible water-alternating-gas (WAG) injection scheme is more effective than waterflooding or gas injection alone. In Section 5 we gather the main conclusions and anticipate ongoing and future work.

2 The front-tracking algorithm

Front-tracking is an algorithm for constructing exact or approximate solutions to hyperbolic systems of conservation laws with general initial data (Cauchy problem):

$$\partial_t u + \partial_x f(u) = 0, \qquad u(x,0) = u_0(x). \tag{1}$$

The algorithm starts from a piecewise constant function $u_0(x)$. Each discontinuity defines a local Riemann problem, where each Riemann problem again is connected to its nearest neighbors through common constant states. All Riemann problems produce a similarity solution, called a Riemann fan, which consists of constant states separated by simple waves with finite speed of propagation. Neighboring Riemann fans can therefore be connected through the common constant state and this way define a global solution in space, which is well defined up to the first time two simple waves interact. If the interacting waves are discontinuities, i.e., shocks or contacts, the interaction defines a new Riemann problem. By solving the Riemann problem and inserting the corresponding local Riemann fan, the global solution can be extended in time until the next interaction and so on (see **Figure 1**). If all simple waves are discontinuities, we can hence have an algorithm for building the global solution of the Cauchy problem.

For systems admitting continuous simple waves (rarefactions), one can similarly construct an *approximate* solution to the Cauchy problem by the above algorithm. To do so, one simply approximates each rarefaction fan by a set of constant states separated by space-time rays of discontinuity. This can be done by sampling states along the integral curve and assigning each discontinuity an appropriate wave-speed; e.g., the Rankine–Hugoniot velocity, or the eigenvalue at the left or right state. Alternatively, one can discretize the wave speeds in the Riemann fan and then obtain the corresponding constant states.

It is also common to perform some kind of data reduction to reduce the number of tracked discontinuities. In the current implementation, we do data reduction on three levels. We ignore

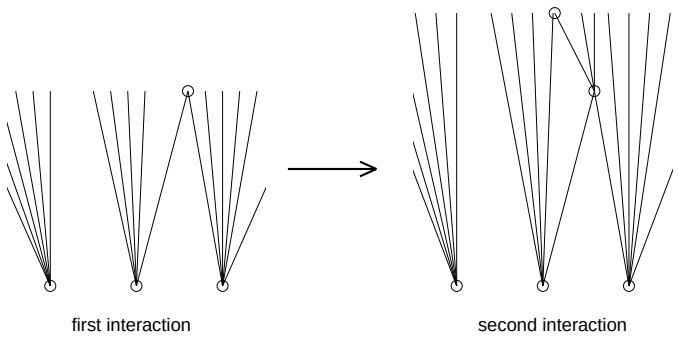

Figure 1. Construction of a global solution by connecting local Riemann fans depicted in the (x,t)-plane.

individual waves that are sufficiently small, for example, in a solution of type $\mathcal{S}$-$\mathcal{C}$-$\mathcal{S}$, we may ignore the last S-wave if it is sufficiently weak. If the difference in left and right states in a Riemann problem is below a certain threshold, the Riemann fan is approximated by a single discontinuity traveling with a wave speed equal the average of the two eigenvalues of the left state. If the difference in states is even smaller, the Riemann problem is simply neglected. This data reduction introduces a (small) error in the mass conservation that can be controlled by picking appropriate threshold values.

To sum up, the front-tracking algorithm consists of the following three key points: solution of Riemann problems, approximation of Riemann fans in terms of step functions, and tracking of discontinuities (fronts). The algorithm is usually realized in the form of a spatially-ordered list of front objects representing each discontinuity and the associated constant states and some priority queue for keeping track of colliding fronts. The front-tracking algorithm is outlined in more detail in Algorithm 1. The basic data objects are the propagating fronts. Each front object f has an associated left and right state, a point of origin, a propagation speed, and a termination point. To track the fronts, we use two lists, a spatial list F where the fronts are sorted from left to right and a collision list C where front collisions are sorted with respect to collision time in ascending order.

3 One-dimensional simulations

In this section we present several simple examples to demonstrate the behavior of the front-tracking algorithm. We have chosen a simple model with quadratic relative permeabilities:

$$k_{rw}(S) = \begin{cases} 0 & \text{if } S < S_{wc} = 0.2, \\ \left(\dfrac{S - S_{wc}}{1 - S_{wc}}\right)^2 & \text{otherwise,} \end{cases} \tag{2}$$

$$k_{rh}(S) = \begin{cases} 0 \quad \text{if } 1 - S < S_{hc} = 0.2, \\ 0.1\left(\dfrac{1 - S - S_{hc}}{1 - S_{hc}}\right) + 0.9\left(\dfrac{1 - S - S_{hc}}{1 - S_{hc}}\right)^2, \end{cases} \tag{3}$$

Algorithm 1 The front-tracking algorithm

Construct a piecewise constant initial function $u_0(x) = u_i$
Set $\mathsf{F} = \{\emptyset\}$, $\mathsf{C} = \{\emptyset\}$, and $t = 0$
For $i = 0 : n$
  $\{\mathsf{f}_L, \ldots, \mathsf{f}_R\} = \text{RiemannSolver}(u_i, u_{i+1}, x_{i+1/2}, t)$
  $\mathsf{c} = \text{ComputeCollision}(\mathsf{F}, \mathsf{f}_L)$
  $\mathsf{C} = \text{Sort}(\{\mathsf{C}, \mathsf{c}\})$
  $\mathsf{F} = \text{InsertFronts}(\{\mathsf{F}, \{\mathsf{f}_L, \ldots, \mathsf{f}_R\})$
While $(t \le T)$ and $\mathsf{C} \neq \{\emptyset\}$ do
    $(\mathsf{c}, x_c, t_c) = \text{ExtractNextCollision}(\mathsf{C})$
    $\{\mathsf{f}_L, \ldots, \mathsf{f}_R\} = \text{ExtractCollidingFronts}(\mathsf{F},\mathsf{c})$
    $\{\mathsf{f}_L, \ldots, \mathsf{f}_R\} = \text{RiemannSolver}(\mathsf{f}_L \to u_L, \mathsf{f}_R \to u_R, x_c, t_c)$
    $\{\mathsf{c}_L, \mathsf{c}_R\} = \text{ComputeCollision}(\mathsf{F}, \{\mathsf{f}_L, \ldots, \mathsf{f}_R\})$
    $\mathsf{C} = \text{Sort}(\{\mathsf{C}, \mathsf{c}_L, \mathsf{c}_R\})$
    $\mathsf{F} = \text{InsertFronts}(\mathsf{F}, \{\mathsf{f}_L, \ldots, \mathsf{f}_R\})$
endwhile

and viscosities given by the quarter-power rule:

$$\mu_h(\chi) = \left[\frac{1-\chi}{\mu_o^{1/4}} + \frac{\chi}{\mu_g^{1/4}} \right]^{-4}, \tag{4}$$

with

$$\mu_w = 1.0, \qquad \mu_o = 4.0, \qquad \mu_g = 0.4.$$

3.1 Example 1

The first example is a simple Riemann problem at $x = 0.1$ with left state $u_l = (0.8, 0)$ and right state $u_r = (0.2, 0.7)$. The left state lies on the border of the region of residual oil, where both eigenvalues are zero. In this case the $\mathcal{R}_2$ region covers the whole saturation triangle. The solution is therefore of the form $u_l \xrightarrow{\mathcal{C}} u_m \xrightarrow{\mathcal{S}} u_r$ and consists of a composite S-rarefaction-shock followed by a C-contact. **Figure 2** shows approximate solutions obtained using two different tolerances for sampling the rarefactions, $\delta_u = 0.01$ and $\delta_u = 0.001$. Whilst the accuracy of the rarefaction is different, the shock and contact are represented exactly in both simulations.

3.2 Example 2

The second example is a simple Riemann problem at $x = 0.1$ with left state $u_l = (0.2, 0.7)$ and right state $u_l = (0.7, 0.2)$. The left state lies in the $\mathcal{L}$ region with $\nu_s = 0 < \nu_c = 1.25$, and the right state lies in the $\mathcal{L}_3$ region. The solution is therefore of the form $u_l \xrightarrow{\mathcal{S}} u_m^{(1)} \xrightarrow{\mathcal{C}} u_m^{(2)} \xrightarrow{\mathcal{S}} u_r$ and consists of a fast composite S-rarefaction-shock followed by a C-contact and a slow S-rarefaction. **Figure 3** shows two approximate solutions obtained using $\delta_u = 0.01$ and $\delta_u = 0.001$.

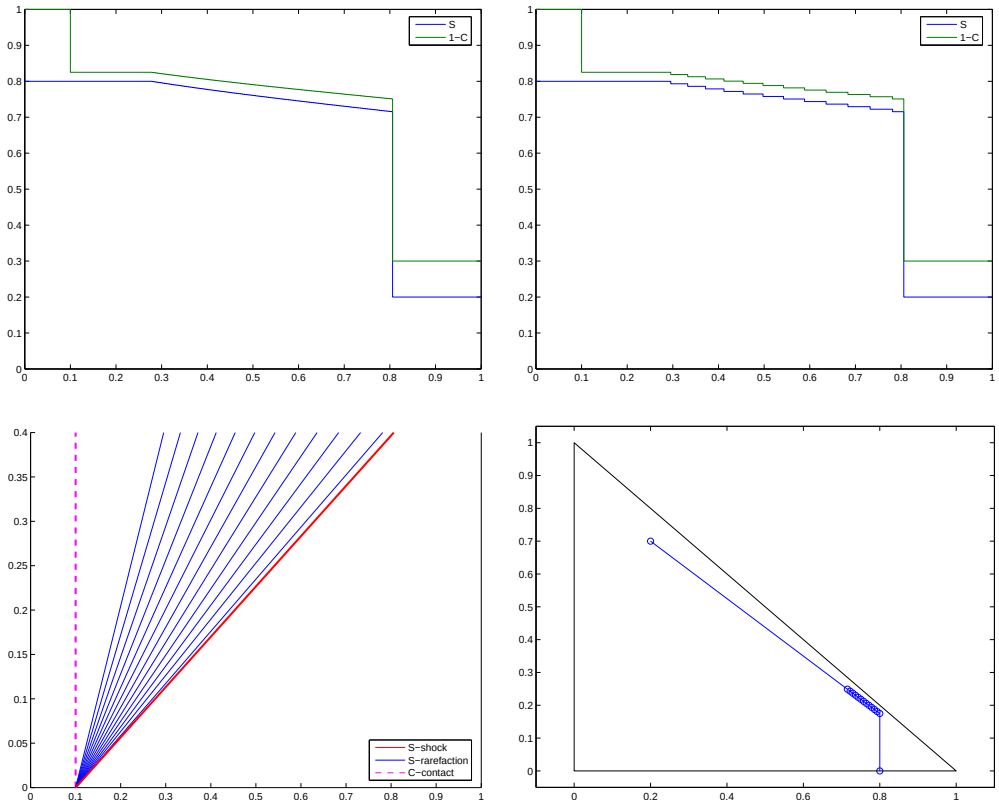

Figure 2. (Example 1) Approximate solutions for $\delta_u = 0.001$ (upper left) and $\delta_u = 0.01$ (upper right), fronts in (x,t)-space (lower left), and solution in saturation triangle (lower right).

3.3 Example 3

In this example we demonstrate the effects of data reduction. To this end, consider the unit interval $x \in [0,1]$ with periodic boundary conditions and an initial Riemann problem with $u_l = (0.1, 0.8)$ and $u_r = (0.8, 0.1)$. We compute the solution up to time $t = 0.75$ in two ways (using $\delta_u = 0.005$):

- Using no data reduction, the simulator solved 89 full Riemann problems.
- Using data reduction when $|u_l - u_r| < 0.01$, 56 full Riemann problems were solved and 19 Riemann problems were approximated by a single wave.

Figure 4 shows the two approximate solutions along with plots of the fronts in the (x,t) plane. We see that the data reduction has been applied to two different sorts of interactions: interaction of a S-rarefaction and the C-contact emanating from $(0, 0.3)$; and interaction of these data-reduced waves and the secondary C-waves produced by the interaction of the S-rarefaction emanating from $(0,0)$ with the fast S-shock emanating from $(0, 0.3)$. The data reduction had little effect on the accuracy since the two approximate solutions are virtually indistinguishable.

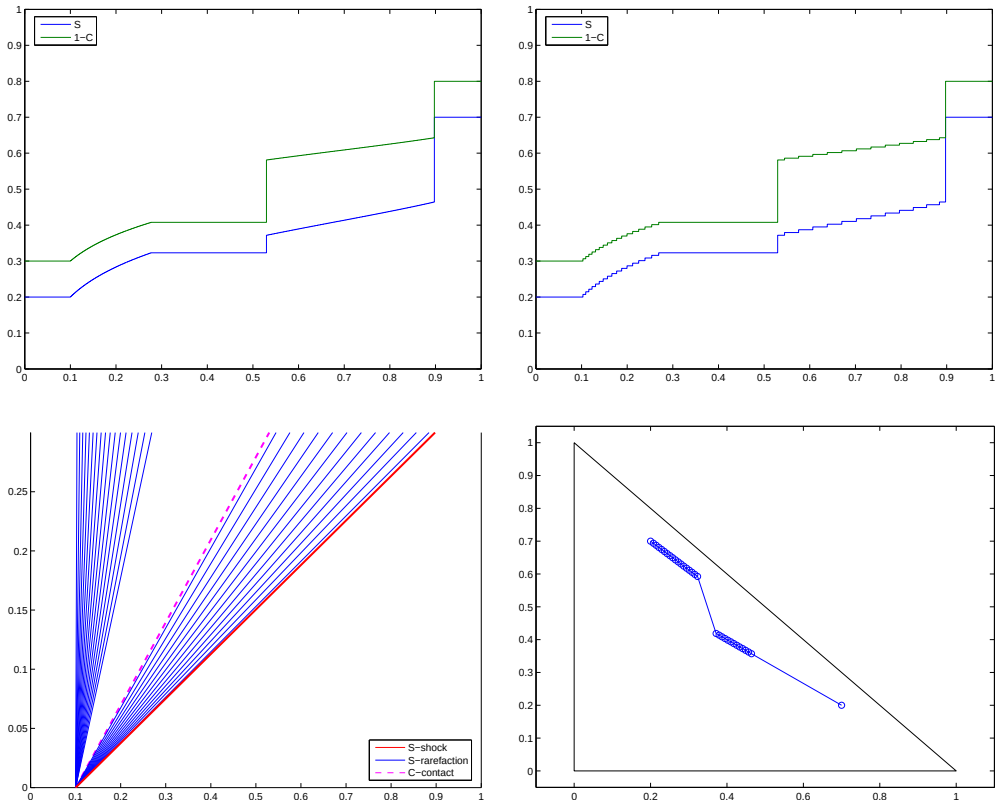

Figure 3. (Example 2) Approximate solutions for $\delta_u = 0.001$ (upper left) and $\delta_u = 0.01$ (upper right), fronts in (x, t)-space (lower left), and solution in saturation triangle (lower right).

3.4 Example 4

Consider now a linear reservoir of length $L = 2$ initially filled with a fluid of composition $(0.3, 0)$. To produce the reservoir four different strategies were proposed:

1. Continuous water injection.
2. Continuous solvent (gas) injection.
3. Alternating solvent and water, with periods $\Delta t = 0.2$.
4. Alternating water and solvent, with periods $\Delta t = 0.2$.

Simulations of the four strategies are shown in **Figure 5** to **Figure 8**. The simulation of each of the two first strategies involved one Riemann solution and wave interactions only at the outflow boundary, whereas the simulation of each of the WAG strategies involved about 1700 wave interactions and 450 Riemann solutions.

3.5 Example 5

From a theoretical point of view, the piecewise constant approximation used in front-tracking may be inadequate for nonstrictly hyperbolic systems. Tveito and Winther [16] showed that

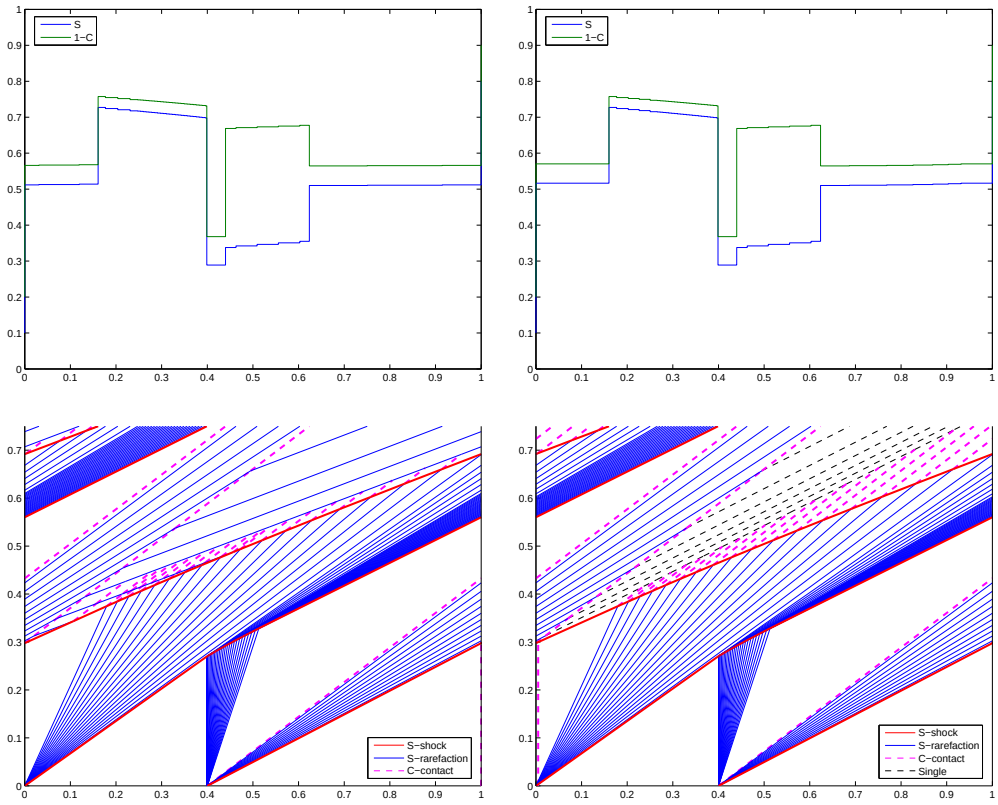

Figure 4. (Example 3) Approximate solutions for $\delta_u = 0.005$ using no data reduction (left column) and approximating Riemann problems for which $|u_l - u_r| < 0.01$ by a single wave (right column).

numerical methods based on a Riemann solver (such as the random choice method and front-tracking) may encounter difficulties for Cauchy problems with initial data on the transition curve due to an initial blowup of the total variation. In this example we show that the miscible flow model has the same property: if initial data on the transition curve $\mathcal{T}$ is approximated by a piecewise constant function, the total variation of the numerical solution at time $t = 0^+$ approaches infinity as the number of constant states in the approximation of the initial data increases.

Figure 9 shows the front tracking approximations at time $t = 10^{-6}$ for two piecewise approximations with $\Delta x = 1/25$ and $\Delta x = 1/100$, respectively. As can be seen in the figure, a piecewise constant initial approximation changes the qualitative behavior of the solution. Each local Riemann problem has a triangular path in phase space that deviates from the transition curve, resulting in nonphysical spikes. Even though these spikes decrease as the magnitude of the jumps is reduced, the total variation blows up as $\Delta x \to 0$ [16].

From a computational point of view, this deficiency is not necessarily important, unless the spikes prevail and pollute the solution at later times. In **Figure 10** we plot the evolution of the front-tracking solution in phase space for $\Delta x = 1/25$. The spikes are still present in the solution at time $t = 0.2$, but have almost disappeared at time $t = 0.5$. As time evolves, waves from neighboring Riemann problems interact and create secondary waves, which also interact,

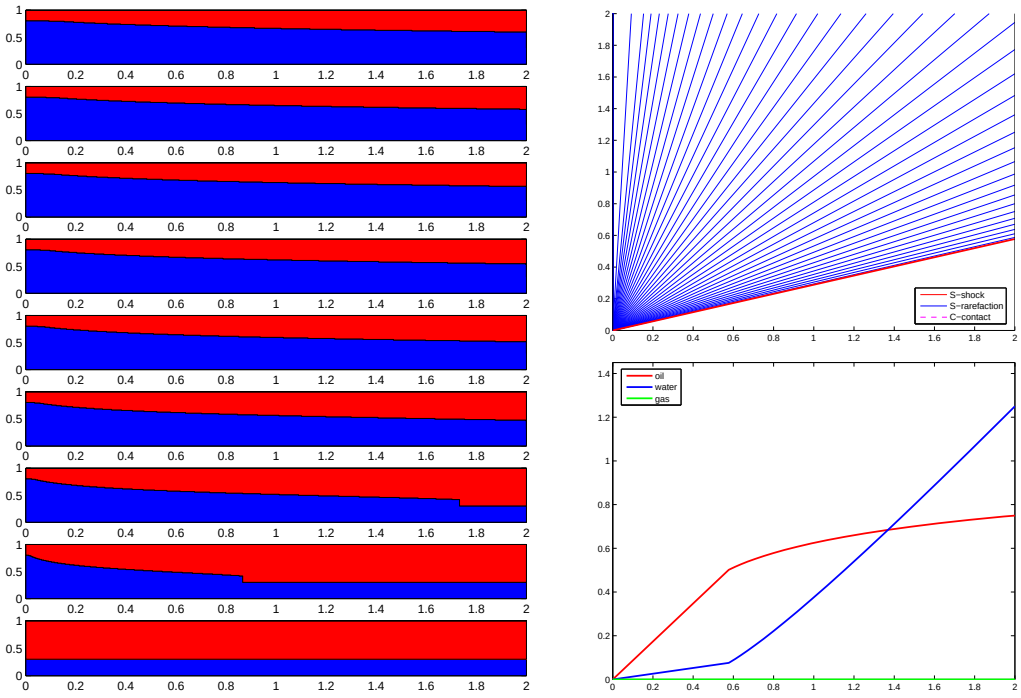

Figure 5. (Example 4) Simulation of water injection. Left column: plot of fluid composition in reservoir at times $t = 0 : 0.25 : 2.0$ from bottom to top. Right column: fronts in (x, t)-plane and cumulative production curves.

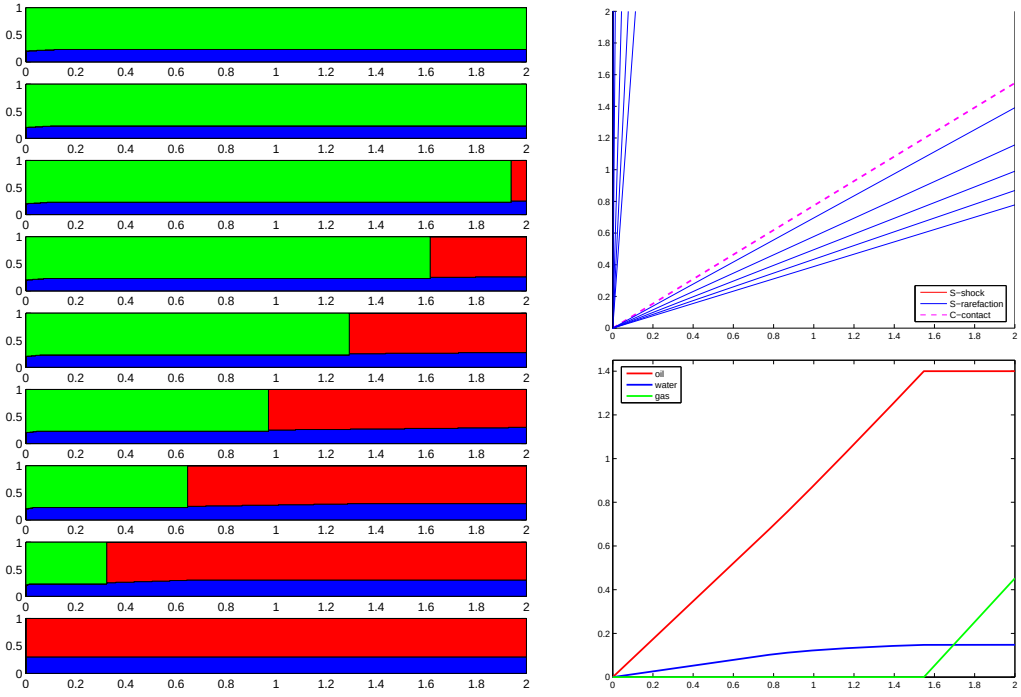

Figure 6. (Example 4) Simulation of solvent injection. Left column: plot of fluid composition in reservoir at times $t = 0 : 0.25 : 2.0$ from bottom to top. Right column: fronts in (x, t)-plane and cumulative production curves.

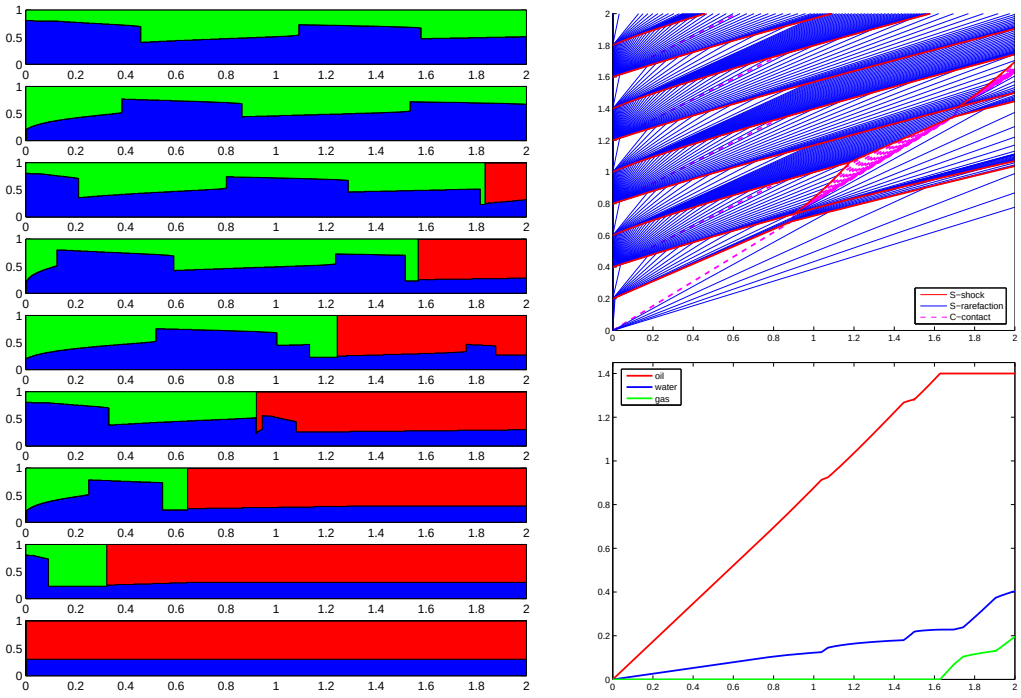

Figure 7. (Example 4) Simulation of alternating water and solvent injection. Left column: plot of fluid composition in reservoir at times $t = 0 : 0.25 : 2.0$ from bottom to top. Right column: fronts in (x, t)-plane and cumulative production curves.

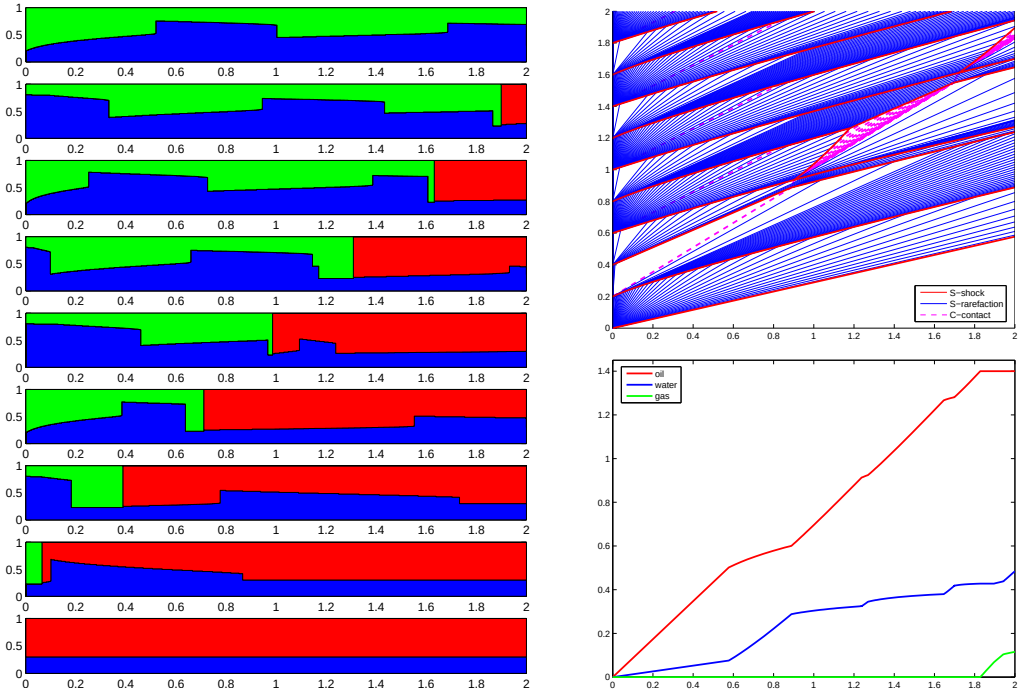

Figure 8. (Example 4) Simulation of alternating solvent and water injection. Left column: plot of fluid composition in reservoir at times $t = 0 : 0.25 : 2.0$ from bottom to top. Right column: fronts in (x, t)-plane and cumulative production curves.

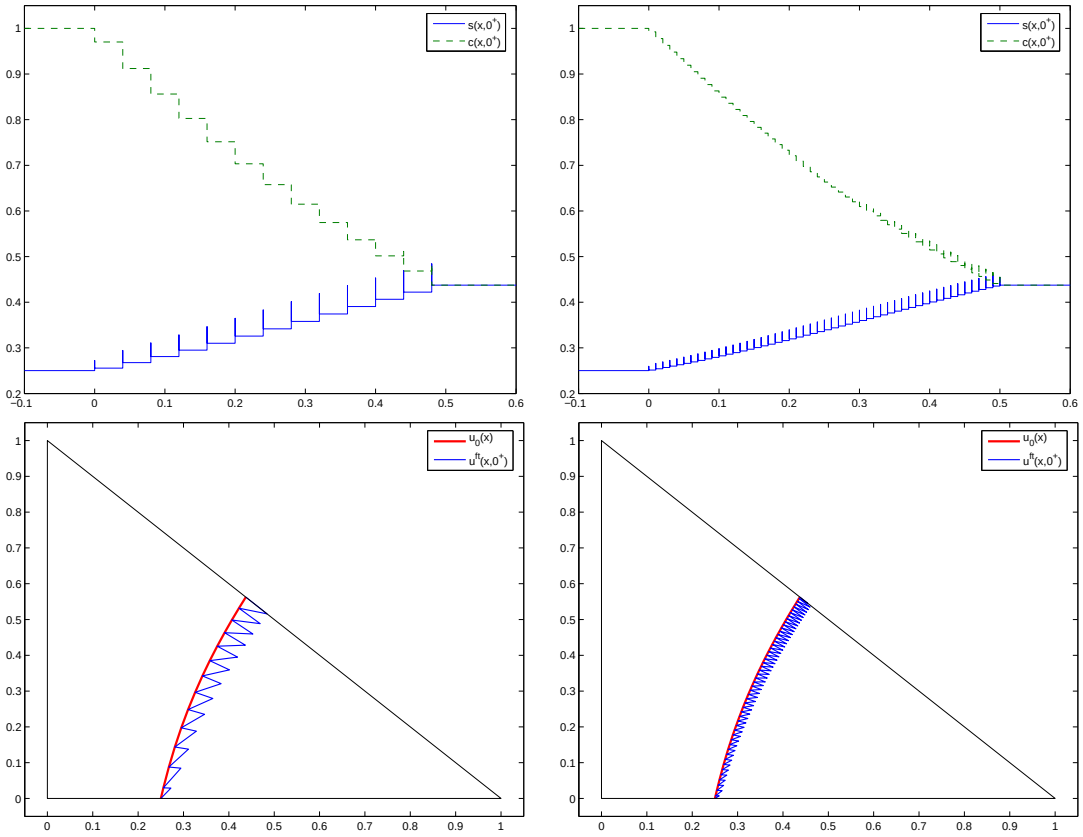

Figure 9. Front tracking approximation of the saturation and concentration at time $t = 10^{-6}$ for the Cauchy problem with initial data on the transition curve. The initial function is piecewise contant on a regular grid with $\Delta x = 1/25$ (left) and $\Delta x = 1/100$ (right).

and so on. For each interaction, the total variation in the solution decreases, see **Table 1**. The oscillations decay faster with smaller Δx.

In summary, initial data on the transition curve may introduce small-scale oscillations and an increased number of wave interactions, but does not prevent the front-tracking algorithm from converging to the true solution at later times. Moreover, if the front-tracking algorithm is combined with repeated projections onto an underlying grid, as will be the case for the streamline simulations discussed in the next section, the numerical solution will leave the transition curve as a combined effect of projections and local wave interactions.

4 Streamline Simulations

The front-tracking method can be used as part of a streamline solver to simulate multidimensional miscible gas displacements. In a multidimensional setting, one needs to solve the pressure equation,

$$\nabla \cdot \boldsymbol{v}_T = 0, \qquad \boldsymbol{v}_T = -\frac{\boldsymbol{k}}{\phi}\lambda_T \nabla p, \tag{5}$$

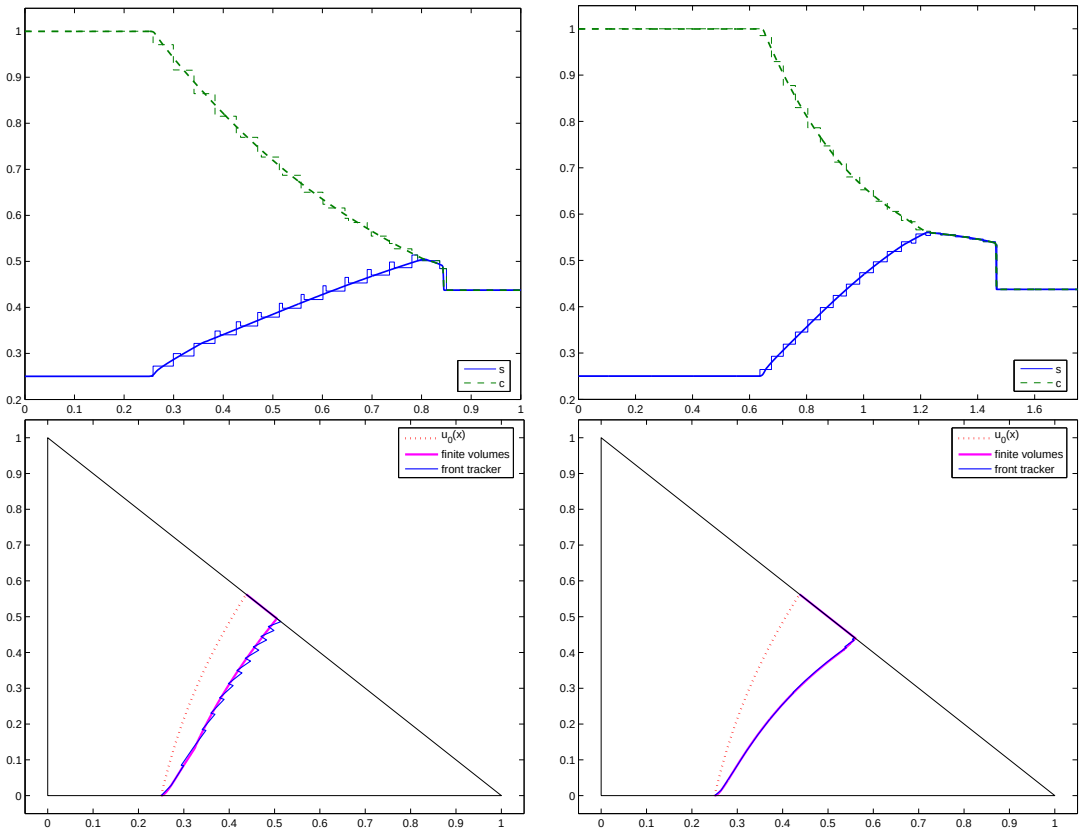

Figure 10. The evolution of the approximate solutions in phase space for times $t = 0.2$ (left) and $t = 0.5$ (right) computed with front tracking using a piecewise constant intial function with $\Delta x = 1/25$

Table 1. Total variation of the front-tracking solution as a function of time and discretization parameter $\Delta x = 1/N$ for the initial approximation.

$t \setminus N$	25	50	100	200	400
10^{-6}	1.8561	2.3501	3.2175	4.4518	6.2497
0.10	1.8561	1.3441	1.3951	1.4236	1.4055
0.20	1.1245	1.1178	1.1237	1.1203	1.1204
0.30	1.0473	1.0403	1.0424	1.0428	1.0428
0.40	1.0164	1.0159	1.0153	1.0151	1.0150
0.50	1.0073	1.0062	1.0061	1.0061	1.0061
0.60	1.0058	1.0054	1.0054	1.0054	1.0054

together with the multidimensional system of transport equations,

$$\frac{\partial S}{\partial t} + \boldsymbol{v}_T \cdot \nabla f = 0, \tag{6}$$

$$\frac{\partial C}{\partial t} + \boldsymbol{v}_T \cdot \nabla \left(\frac{1-f}{1-S} C \right) = 0. \tag{7}$$

The pressure equation (5) and the system of transport equations (6)–(7) are coupled due to the dependence of the total mobility λ_T on the water saturation S and the overall solvent concentration C. The streamline solver is based on an operator splitting strategy consisting of the following two steps:

1. *Pressure step.* Water saturation and solvent concentration are frozen and their values are assigned to each gridblock of a fixed (background) grid where the permeability and porosity are defined. The (elliptic) pressure equation is solved using, for example, a finite difference method. The total velocity $\boldsymbol{v}_T$ is computed, and streamlines are then traced covering the domain of interest—usually emanating from injection wells and arriving at production wells. Individual streamlines are parameterized by the time-of-flight $\tau = \tau(\boldsymbol{x})$ that measures the travel time for a passive particle released at the boundary (i.e., an injection well) to reach a point $\boldsymbol{x}$ in the domain. In the simulator, streamline tracing and time-of-flight computations are carried out using an analytic method developed by Pollock [17].

2. *Transport step.* The three-dimensional transport equations are solved as a set of decoupled one-dimensional equations along streamlines. Values of water saturation and solvent concentration are mapped from the background grid to the streamline grid, defining a Cauchy problem on each streamline. Saturations and concentrations are evolved in time by means of the front-tracking algorithm for a user-specified time step. Once this target time is reached, the streamline saturations and compositions are projected back onto the background grid.

Each saturation step typically involves several thousand streamlines, resulting in a very large number of calls to the Riemann solver. A key point in obtaining an efficient solver is therefore to use the data-reduction algorithm illustrated in Example 3 to reduce the number of calls to the Riemann solver. Details about the implementation of a front-tracking algorithm within a streamline simulation framework are described elsewhere (see, e.g. [8; 12; 18]), and will be omitted here.

4.1 Quarter five-spot simulations in a homogeneous reservoir

We present results using the numerical method described above for the simulation of pure solvent injection in a two-dimensional homogeneous reservoir initially filled with 70% oil and 30% water. The injection and production wells follow a repeated five-spot pattern, and the simulations are carried out with grids representing one quarter of a pattern, in which injector and producer are located in diagonally opposite vertices of the grid (**Figure 11**).

The mathematical model does not contain diffusive terms and, therefore, the problem is physically unstable and mathematically ill-posed. Unique numerical solutions are obtained because of

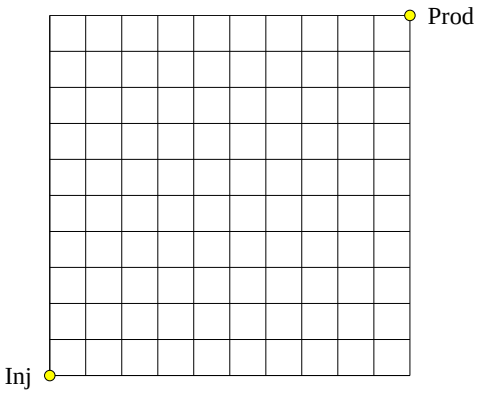

Figure 11. Schematic of a 10×10 grid for the homogeneous quarter five-spot problem.

the stabilizing diffusive effects introduced by any numerical method. As a result, the numerical solution is to a large extent determined by the artificial diffusion introduced by the computational scheme. This issue of grid refinement and grid orientation effects has been studied at length in the context of finite difference methods [19; 20] and has motivated the application of high-order finite difference schemes to the simulation of miscible displacements [21].

In streamline simulation, the are several sources of numerical diffusion:

1. Mapping from the finite difference grid to the streamlines to initialize a new transport step. The mapping error is proportional to the gridblock size Δx.

2. Mapping from the streamline grid to the background grid at the end of the transport step. The mapping error is in fact a sampling error, and decreases as the number of streamlines is increased.

3. Numerical diffusion along streamlines, which we avoid completely by the use of a front-tracking algorithm.

Since the level of numerical diffusion depends on the grid resolution (gridblock size, time step between pressure updates, and number of streamlines), the numerical solution is necessarily grid dependent. The expectation, however, is that front-tracking/streamline methods exhibit less grid dependence than traditional, first-order finite difference methods [22; 23].

In **Figure 12** and **Figure 13** we show maps of water saturation and solvent concentration after 2000 days of injection, respectively, computed on increasingly refined grids. The time step between pressure updates was kept constant and equal to 50 days. The number of streamlines employed increases with the grid resolution, in order to guarantee that the sampling error from the streamline grid to the background grid is much smaller than the numerical diffusion due to the mapping error from the background grid to the streamline grid. It is apparent that the solution is grid dependent, because the stabilizing mechanism is the diffusion due to mapping from background grid to streamline grid, which is proportional to Δx.

The evolution of the water, oil and solvent cuts (fractional flows at the production well) are shown in **Figure 14** for the different grids used. As expected —and in accordance with the saturation and concentration maps shown in Figures 12 and 13— the recovered fractional flows

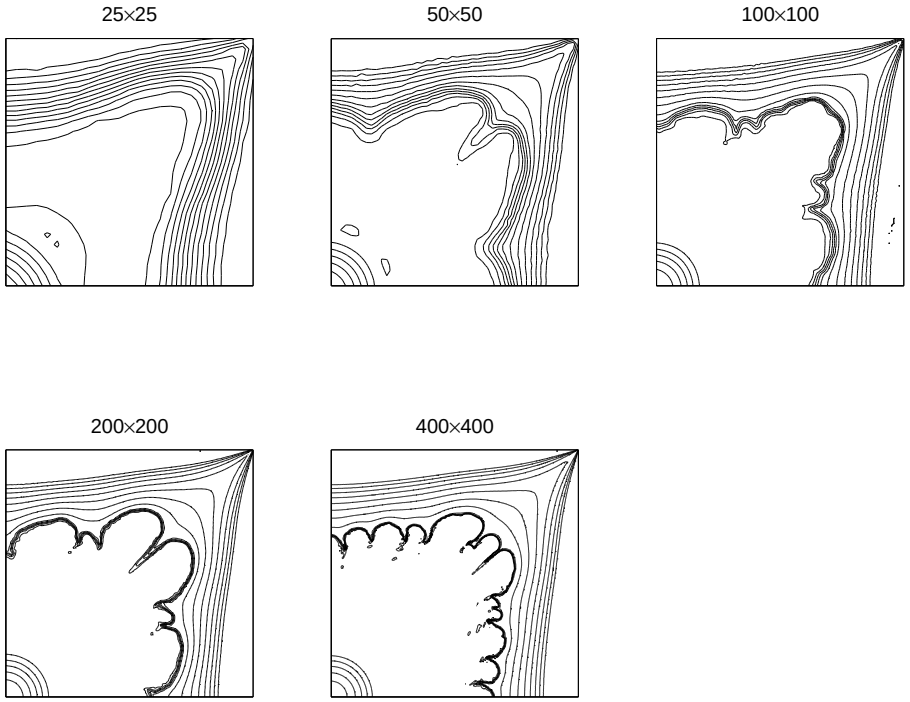

Figure 12. Water saturation maps at $t = 2000$ days for the quarter five-spot problem using increasingly refined grids.

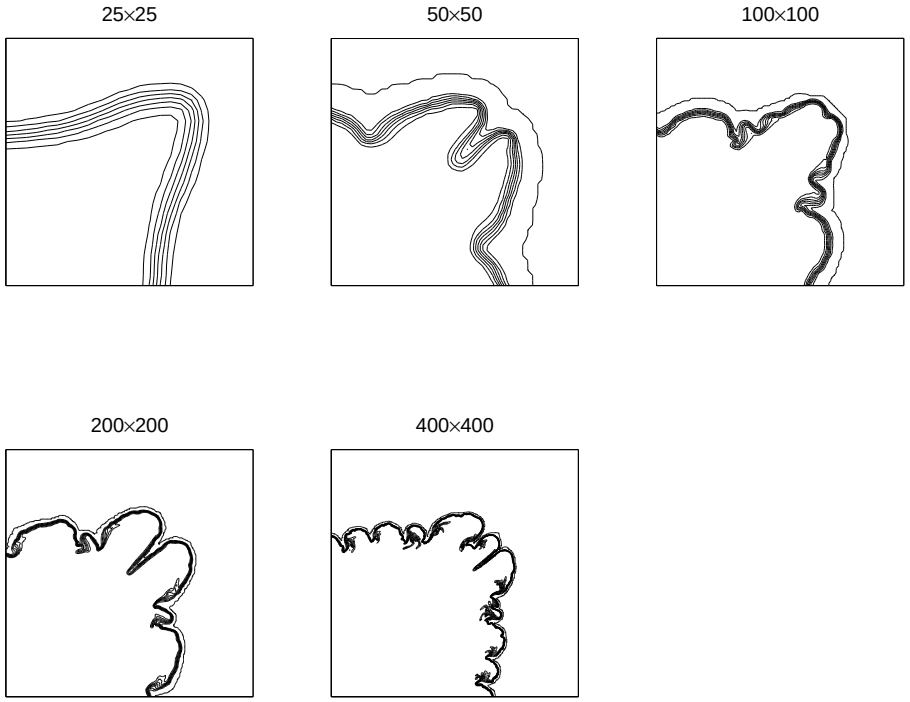

Figure 13. Solvent concentration maps at $t = 2000$ days for the quarter five-spot problem using increasingly refined grids.

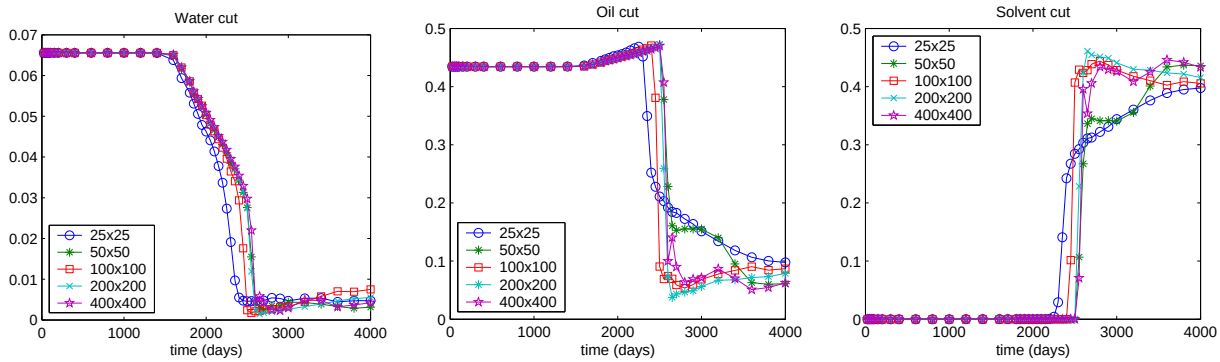

Figure 14. Water, oil and solvent cuts for the quarter five-spot problem with increasingly refined grids.

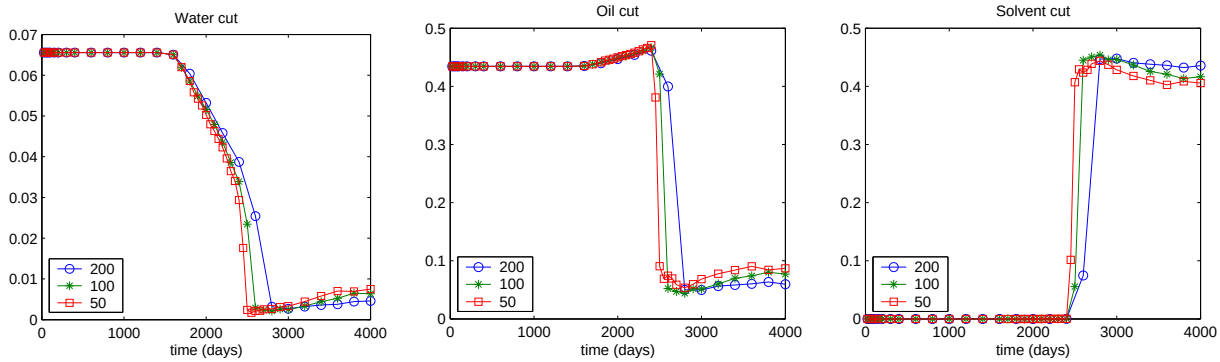

Figure 15. Water, oil and solvent cuts for the quarter five-spot problem with increasingly refined time step between pressure updates.

do not display true convergence. These curves, however, are far less sensitive to grid refinement than those obtained with first-order finite difference methods [21].

Similar observations apply if we investigate the effect of the time step between pressure updates. In this case, numerical diffusion is actually increased as the time step is refined due to the increased number of mappings between the streamline and finite difference grids. The water, oil and solvent cuts computed on a 100×100 grid for time steps of 200, 100 and 50 days are shown in **Figure 15**. Although the solutions cannot be regarded as truly converged numerical solutions, they are not very sensitive to the choice of the time step.

Finally, we demonstrate that the front-tracking/streamline method does converge with respect to the number of streamlines. In **Figure 16** we show the produced fractional flow curves computed on a 100×100 grid and a time step of 50 days between pressure updates, with different number of streamlines. Clearly, the solutions converge as the number of streamlines is increased. The reason is that the sampling error from the streamline grid to the background grid is minimized, and the numerical diffusion comes entirely from the forward mapping from the background grid onto the streamlines.

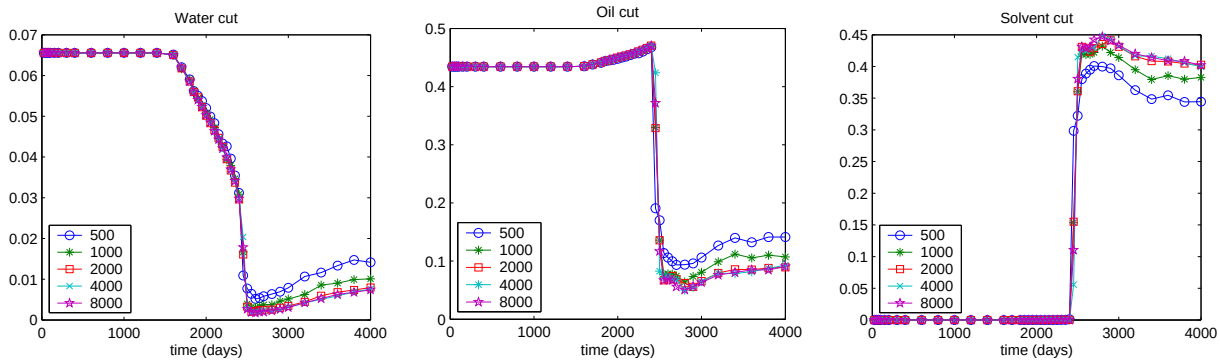

Figure 16. Water, oil and solvent cuts for the quarter five-spot problem computed on a 100×100 grid with a time step of 50 days and increasing number of streamlines.

4.2 Three-dimensional simulations in a heterogeneous reservoir

We consider a three-dimensional rectangular reservoir model consisting of a subsample ($30 \times 110 \times 15$ gridblocks) of the highly heterogeneous shallow-marine Tarbert formation from the 10th SPE comparative solution project [24]. The permeability varies six orders of magnitude in the horizontal and ten orders of magnitude in the vertical direction, see **Figure 17**. The porosity is strongly correlated to the permeability. The reservoir is initially filled with 70% oil and 30% water, $(S, C) = (0.3, 0)$, and for simplicity we neglect gravity and assume incompressible flow.

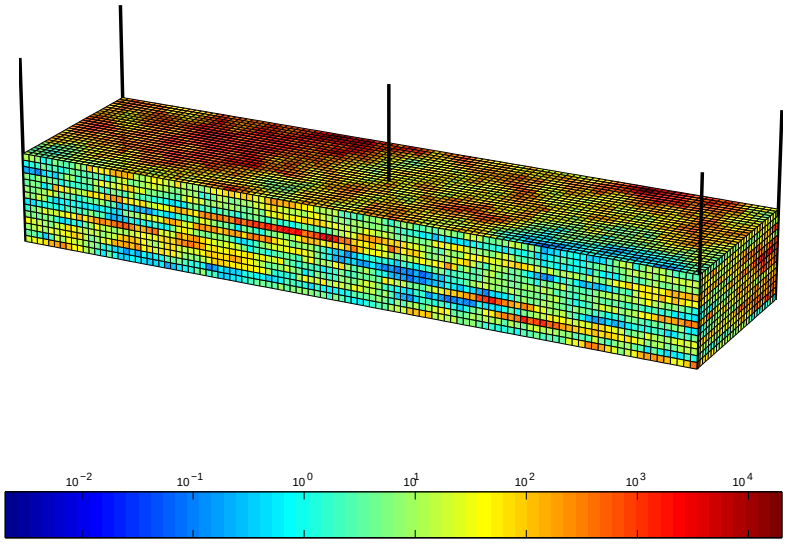

Figure 17. Horizontal permeability and well configuration for the Tarbert formation.

To produce the reservoir, we introduce a five-spot well configuration with one vertical injection well in the center and four vertical producers at the corners, and consider three different production scenarios: (i) injection of pure water, i.e., $(S, C) = (1, 0)$; (ii) injection of pure solvent, i.e., $(S, C) = (0, 1)$; and (iii) a WAG cycle where the injected fluid composition is changed between pure water and pure solvent every 200 days, starting at day 400. In **Figure 18** we show

three-dimensional maps of the solvent concentration C after 800 days of injection for the pure solvent injection case (top) and the WAG injection case (bottom). The solutions were obtained using 10,000 streamlines and a time step between pressure updates of 200 days for the water injection and solvent injection cases, and 25 days for the WAG case.

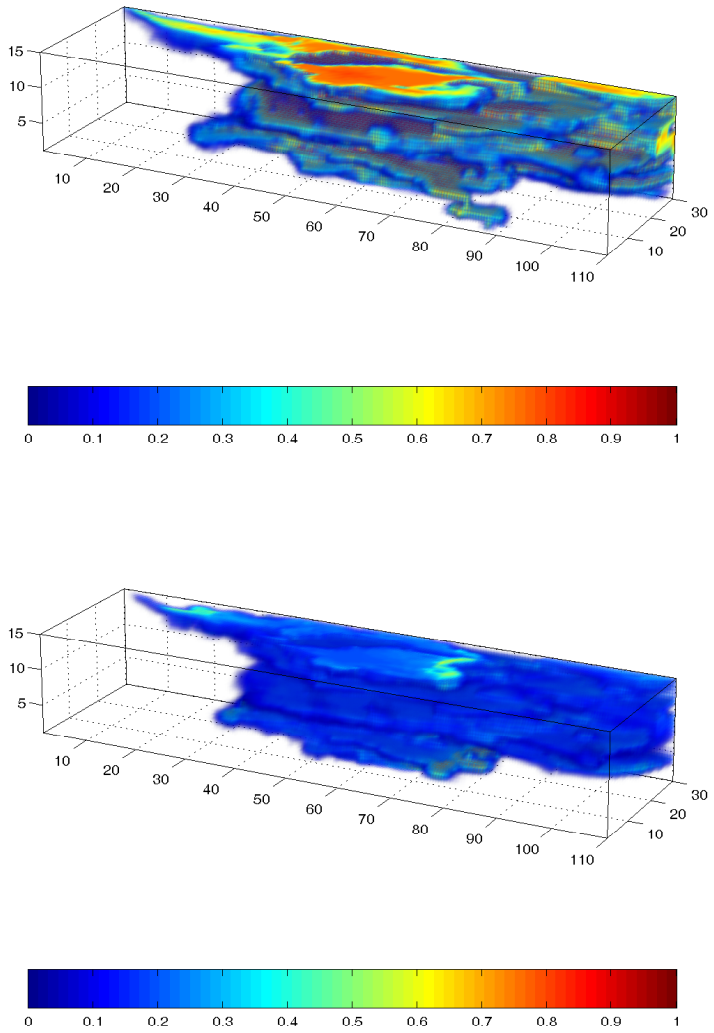

Figure 18. Map of the solvent concentration in the Tarbert formation after 800 days for continuous solvent injection (top) and water-alternating-gas injection (bottom).

We compare the predictions of the streamline/front-tracking simulations with an industry-standard finite difference simulator, Eclipse 100 [25]. The first-contact miscible (FCM) option was used with a value of the Todd and Longstaff parameter $\omega = 1$ to suppress the effects of viscous fingering. Eclipse was run in fully implicit mode with adaptive time-step control, and using a nine-point stencil (in the areal dimension) to reduce grid orientation effects characteristic of high mobility ratio miscible displacements. In **Figure 19** we show a comparison of the oil, water and solvent production curves for 2000 days of production for all three scenarios. Eclipse results are

plotted with solid lines, and streamline/front-tracking results with dashed lines. The agreement between the two codes is excellent for the water injection case, and this is consistent with previous findings for *immiscible* three-phase flows [12]. Although in fair agreement, the finite difference and the streamline/front-tracking solutions show noticeable differences for the WAG injection and solvent injection cases. The finite difference solution predicts slightly earlier breakthrough of the injected solvent to the production well, and slightly higher recovery overall. A plausible explanation for this behavior is that the finite difference scheme introduces numerical diffusion (not present in the physical model), which causes the injected solvent to contact more of the initial oil, thereby predicting a shorter travel time between injector and producer as well as an enhanced sweep efficiency. Artificial diffusion is also introduced in the streamline simulations every time the pressure field is updated, due to the necessary remapping of saturations and concentrations from the streamlines back to the finite difference grid. On the other hand, the front-tracking method does not introduce *any* numerical diffusion during the evolution of saturations and concentration along streamlines. For the time step between pressure updates chosen, it seems apparent that the artificial diffusive effects of the streamline simulations are smaller than those of the finite difference simulations.

An interesting practical observation from the simulations shown above is that the recovery efficiency of the WAG scheme is higher than that of either water injection and gas injection alone, even though no attempt was made to optimize the WAG ratio or slug size.

5 Conclusions

In this series of two papers we have presented an efficient computational framework for the simulation of first-contact miscible gas injection processes. The framework is based on three key technologies: (1) a streamline method that decouples the three-dimensional transport equations into a set of one-dimensional problems along streamlines; (2) a front-tracking algorithm for the accurate (or even exact) solution of general one-dimensional initial and boundary-value problems; and (3) an analytical Riemann solver for the first-contact miscible system, used as a building block in the front-tracking method.

The mathematical model and the analytical Riemann solver were described in Part 1, and used here within a front-tracking/streamline framework that exploits the markedly different character of the governing equations: an elliptic pressure equation, and a hyperbolic system of transport equations. The integration of analytical Riemann solvers, the front-tracking method, and streamline tracing, offers the potential for fast and accurate prediction of miscible gas and WAG injection in real reservoirs. In this paper, several representative examples are used to illustrate the excellent behavior of the front-tracking method. In particular, we present an application of this computational framework for the simulation of miscible flooding in a three-dimensional, highly heterogeneous formation, and demonstrate that a miscible water-alternating-gas injection scheme is more efficient than waterflooding or gas injection alone. Although this was not pursued here, this fast computational tool could have been used in an optimization loop for designing optimal WAG schemes (e.g., WAG ratio and slug size).

The application of the proposed computational approach to real reservoir simulation studies requires several extensions, such as accounting for viscous fingering effects [26–28] and the ability to handle regions with different relative permeability functions [29; 30]. Other physical processes,

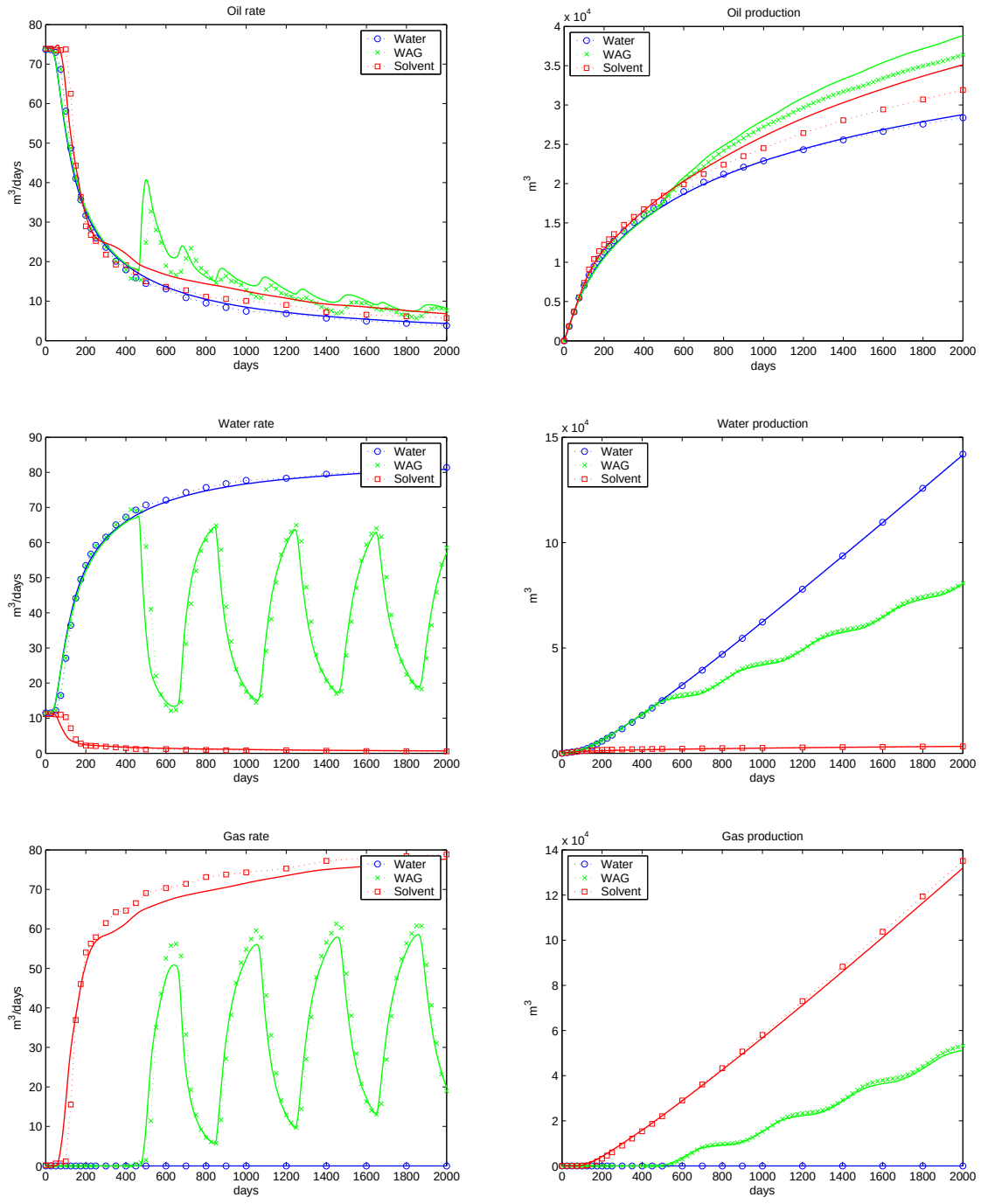

Figure 19. Rates and cumulative production curves for water, solvent and WAG injection for the Tarbert formation. Eclipse results are shown with solid lines; streamline/front-tracking results are shown with dashed lines.

such as gravity, capillarity, and compressibility, should also be incorporated into the streamline simulator.

Acknowledgements

R.J. gratefully acknowledges financial support from the industrial affiliates of the Stanford University Petroleum Research Institute for Numerical Simulation (SUPRI-B) and Gas Injection (SUPRI-C). K.-A.L. gratefully acknowledges financial support from the Research Council of Norway under grant number 158908/I30.

References

[1] R. Juanes and K.-A. Lie. Numerical modeling of multiphase first-contact miscible flows. Part 1. Analytical Riemann solver. *Transp. Porous Media*, 2005. (Submitted).

[2] E. L. Isaacson. Global solution of a Riemann problem for a non-strictly hyperbolic system of conservation laws arising in enhanced oil recovery. Technical report, The Rockefeller University, New York, 1980.

[3] T. Johansen and R. Winther. The solution of the Riemann problem for a hyperbolic system of conservation laws modeling polymer flooding. *SIAM J. Math. Anal.*, 19(3):541–566, 1988.

[4] H. Holden and N. H. Risebro. *Front Tracking for Hyperbolic Conservation Laws*, volume 152 of *Applied Mathematical Sciences*. Springer, New York, 2002.

[5] N. H. Risebro. A front-tracking alternative to the random choice method. *Proc. Amer. Math. Soc*, 117(4):1125–1129, 1993.

[6] A. Bressan and P. LeFloch. Uniqueness of weak solutions to systems of conservation laws. *Arch. Rational Mech. Anal.*, 140(4):301–317, 1997.

[7] N. H. Risebro and A. Tveito. A front tracking for conservation laws in one dimension. *J. Comput. Phys.*, 101(1):130–139, 1992.

[8] F. Bratvedt, K. Bratvedt, C. F. Buchholz, T. Gimse, H. Holden, L. Holden, and N. H. Risebro. Frontline and Frontsim, two full scale, two-phase, black oil reservoir simulators based on front tracking. *Surv. Math. Ind.*, 3:185–215, 1993.

[9] N. H. Risebro and A. Tveito. Front tracking applied to a nonstrictly hyperbolic system of conservation laws. *SIAM J. Sci. Stat. Comput.*, 12(6):1401–1419, 1991.

[10] R. P. Batycky, M. J. Blunt, and M. R. Thiele. A 3D field-scale streamline-based reservoir simulator. *SPE Reserv. Eng.*, 11(4):246–254, 1997.

[11] M. J. King and A. Datta-Gupta. Streamline simulation: A current perspective. *In Situ*, 22(1):91–140, 1998.

[12] K.-A. Lie and R. Juanes. A front-tracking method for the simulation of three-phase flow in porous media. *Comput. Geosci.*, 9(1):29–59, 2005.

[13] R. Juanes, K.-A. Lie, and V. Kippe. A front-tracking method for hyperbolic three-phase models. In *European Conference on the Mathematics of Oil Recovery, ECMOR IX*, volume 2, paper B025, Cannes, France, August 30–September 2 2004.

[14] H. Holden and N. H. Risebro. A method of fractional steps for scalar conservation laws without the CFL condition. *Math. Comp.*, 60(201):221–232, 1993.

[15] V. Haugse, K. H. Karlsen, K.-A. Lie, and J. R. Natvig. Numerical solution of the polymer system by front tracking. *Transp. Porous Media*, 44:63–83, 2001.

[16] A. Tveito and R. Winther. The solution of nonstrictly hyperbolic conservation laws may be hard to compute. *SIAM J. Sci. Comput.*, 16(2):320–329, 1995.

[17] D. W. Pollock. Semianalytical computation of path lines for finite difference models. *Ground Water*, 26:743–750, 1988.

[18] J. E. Aarnes, V. Kippe, and K.-A. Lie. Mixed multiscale finite elements and streamline methods for reservoir simulation of large geomodels. *Adv. Water Resour.*, 28:257–271, 2005.

[19] T. F. Russell and M. F. Wheeler. Finite element and finite difference methods for continuous flows in porous media. In R. E. Ewing, editor, *The Mathematics of Reservoir Simulation*, pages 35–106. SIAM, Philadelphia, PA, 1983.

[20] G. R. Shubin and J. B. Bell. An analysis of the grid orientation effect in numerical simulation of miscible displacements. *Comput. Methods Appl. Mech. Engrg.*, 47:47–71, 1984.

[21] W. H. Chen, L. J. Durlofsky, B. Engquist, and S. Osher. Minimization of grid orientation effects through the use of higher-order finite difference methods. *SPE Advanced Technology Series*, 1:43–52, 1993.

[22] J. Glimm, B. Lindquist, O. A. McBryan, B. Plohr, and S. Yaniv. Front tracking for petroleum reservoir simulation. In *SPE Reservoir Simulation Symposium*, San Francisco, CA, November 15–18 1983. (SPE 12238).

[23] R. E. Ewing, T. F. Russell, and M. F. Wheeler. Convergence analysis of an approximation of miscible displacement in porous media by mixed finite elements and a modified method of characteristics. *Comput. Methods Appl. Mech. Engrg.*, 47(1–2):73–92, 1984.

[24] M. A. Christie and M. J. Blunt. Tenth SPE comparative solution project: A comparison of upscaling techniques. *SPE Reserv. Eval. Eng.*, 4(4):308–317, 2001. url: www.spe.org/csp.

[25] Schlumberger. *Eclipse Technical Description, v. 2003A*, 2003.

[26] M. Blunt and M. Christie. How to predict viscous fingering in three component flow. *Transp. Porous Media*, 12:207–236, 1993.

[27] M. Blunt and M. Christie. Theory of viscous fingering in two phase, three component flow. *SPE Advanced Technology Series*, 2(2):52–60, 1994.

[28] R. Juanes and M. J. Blunt. Analytical solutions to multiphase first-contact miscible models with viscous fingering. *Transp. Porous Media*, 2005. (Accepted).

[29] T. Gimse and N. H. Risebro. Solution of the Cauchy problem for a conservation law with a discontinuous flux function. *SIAM J. Math. Anal.*, 23(3):635–648, 1992.

[30] T. Gimse and N. H. Risebro. A note on reservoir simulation for heterogeneous porous media. *Transp. Porous Media*, 10(3):257–270, 1993.